

Enforced η^1 -Fluorenyl Coordination to Rhodium(I) with the [FluPPh₂NPh][−] Ligand

Christelle Freund,[†] Noémi Barros,[‡] Heinz Gornitzka,[†] Blanca Martin-Vaca,[†]
Laurent Maron,^{*,‡} and Didier Bourissou^{*,†}

Laboratoire Hétérochimie Fondamentale et Appliquée du CNRS (UMR 5069) Université Paul Sabatier,
118 Route de Narbonne, F-31062 Toulouse Cedex 09, France, and LNMO (Laboratoire de Nanophysique,
Magnétisme et Optoélectronique), INSA, Université Paul Sabatier, 135 Avenue de Rangueil,
F-31077 Toulouse Cedex, France

Received June 20, 2006

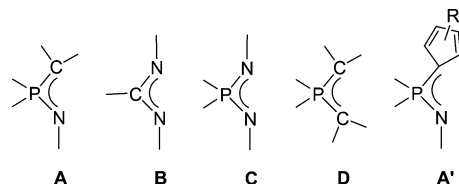
Summary: The fluorenyl-phosphazene ligand **2** has been prepared and coordinated to the Rh^I(nbd) fragment. X-ray analyses and DFT calculations substantiate the preference of the resulting complex **3** for κ^2 -N,C over η^5 -fluorenyl coordination. Despite the associated geometry constraint, the coordination of the short phosphazene sidearm is shown to enforce η^1 -fluorenyl coordination.

Introduction

The coordination properties of 1-aza-2-phospha(V)allyl ligands **A** have attracted considerable interest over the last 15 years (Chart 1).^{1–6} Compared with their 1,3-diaza-allyl (the so-called amidinates) **B**, 1,3-diaza-2-phospha(V)allyl **C**, and 2-phospha(V)allyl **D** analogues, ligands **A** combine two different donor atoms (N and C) and potentially induce electronic as well as steric desymmetrization of the metal environment. Introduction of functional groups on the central NPC skeleton can further influence their coordination properties, as nicely illustrated by the incorporation of an aryl group⁷ or a second phosphinimino group⁸ at carbon or a methoxycarbonyl group at nitrogen.⁹

With this in mind, we recently became interested in the incorporation of the carbon atom of ligands **A** into a Cp-type ring (such as cyclopentadienyl, indenyl, fluorenyl). The resulting ligands **A'** can also be regarded as Cp-type derivatives featuring

Chart 1. Structure of the Heteroallyl Ligands A–D



a phosphazene sidearm, and the presence of this strongly donating pendant group¹⁰ can be expected to influence dramatically the bonding mode of the Cp-type ligand. Here we report the synthesis and structural characterization of a fluorenyl-phosphazene ligand and its ensuing Rh^I(nbd) complex. X-ray analyses and DFT calculations substantiate the preference of this system for κ^2 -N,C over η^5 -fluorenyl coordination.¹¹ Despite the associated geometry constraint, the coordination of the short phosphazene sidearm is shown to enforce η^1 -fluorenyl coordination.¹²

Results and Discussion

The Staudinger reaction appeared a straightforward and efficient route to the desired bifunctional ligand **2**, which was obtained in 56% isolated yield by reacting the readily available fluorenyl-diphenylphosphine **1**¹³ with phenyl azide¹⁴ in toluene at room temperature (Scheme 1). According to ¹H and ¹³C NMR,

* To whom correspondence should be addressed. Fax +33 (0)5 61 55 82 04. Tel +33 (0)5 61 55 77 37. E-mail: dbouriss@chimie.ups-tlse.fr.

[†] Laboratoire Hétérochimie Fondamentale et Appliquée du CNRS.

[‡] LNMO, INSA.

(1) For general reviews, see: (a) Izod, K. *Coord. Chem. Rev.* **2002**, *227*, 153–173. (b) Steiner, A.; Zacchini, S.; Richards, P. I. *Coord. Chem. Rev.* **2002**, *227*, 193–216.

(2) For Li complexes, see: (a) López-Ortiz, F.; Peláez-Arango, E.; Tejerina, B.; Pérez-Carreño, E.; García-Granda, S. *J. Am. Chem. Soc.* **1995**, *117*, 9972–9981. (b) Müller, A.; Neumüller, B.; Dehnicke, K. *Chem. Ber.* **1996**, *129*, 253–257. (c) Hitchcock, P. B.; Lappert, M. F.; Wang, Z.-X. *Chem. Commun.* **1997**, 1113–1114. (d) Hitchcock, P. B.; Lappert, M. F.; Uiterweerd, P. G. H. *J. Chem. Soc., Dalton Trans.* **1999**, 3413–3418. (e) Müller, A.; Neumüller, B.; Dehnicke, K. *Z. Anorg. Allg. Chem.* **2002**, *628*, 100–106. (f) Price, R. D.; Fernández, I.; Ruiz-Gómez, G.; López-Ortiz, F.; Davidson, M. G.; Cowan, J. A.; Howard, J. A. K. *Organometallics* **2004**, *23*, 5934–5938. (g) López-Ortiz, F. *Curr. Org. Synth.* **2006**, *3*, 187–214.

(3) For Zr and Ti complexes, see: (a) Sarsfield, M. J.; Thornton-Pett, M.; Bochmann, M. *J. Chem. Soc., Dalton Trans.* **1999**, 3329–3330. (b) Said, M.; Thornton-Pett, M.; Bochmann, M. *J. Chem. Soc., Dalton Trans.* **2001**, 2844–2849.

(4) For Rh and Ir complexes, see: (a) Imhoff, P.; Nefkens, S. C. A.; Elsevier, C. J.; Goubitz, K.; Stam, C. H. *Organometallics* **1991**, *10*, 1421–1431. (b) Imhoff, P.; van Asselt, R.; Ernsting, J. M.; Vrieze, K.; Elsevier, C. J.; Smeets, W. J. J.; Spek, A. L.; Kentgens, A. P. M. *Organometallics* **1993**, *12*, 1523–1536.

(5) For Ni, Pd, and Pt complexes, see: (a) Avis, M. W.; Vrieze, K.; Kooijman, H.; Veldman, N.; Spek, A. L.; Elsevier, C. J. *Inorg. Chem.* **1995**, *34*, 4092–4105. (b) Avis, M. W.; Vrieze, K.; Ernsting, J. M.; Elsevier, C. J.; Veldman, N.; Spek, A. L.; Katti, K. V.; Barnes, C. L. *Organometallics* **1996**, *15*, 2376–2392. (c) Masuda, J. D.; Wei, P.; Stephan, D. W. *Dalton Trans.* **2003**, 3500–3505.

(6) For Sn, Ge, and Pb complexes, see: (a) Hitchcock, P. B.; Lappert, M. F.; Wang, Z.-X. *J. Organomet. Chem.* **2006**, *691*, 2748–2756. (b) Leung, W. P.; Wong, K. W.; Wang, Z. X.; Mak, T. C. W. *Organometallics* **2006**, *25*, 2037–2044.

(7) Said, M.; Thornton-Pett, M.; Bochmann, M. *Organometallics* **2001**, *20*, 5629–5635.

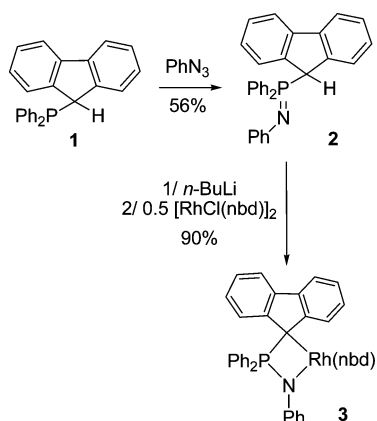
(8) Bibal, C.; Smurnyy, Y. D.; Pink, M.; Caulton, K. G. *J. Am. Chem. Soc.* **2005**, *127*, 8944–8945.

(9) Fernández, I.; Álvarez Gutiérrez, J. M.; Kocher, N.; Leusser, D.; Stalke, D.; González, J.; López-Ortiz, F. *J. Am. Chem. Soc.* **2002**, *124*, 15184–15185.

(10) For selected references, see: (a) Reetz, M. T.; Bohres, E.; Goddard, R. *Chem. Commun.* **1998**, 935–936. (b) Sauthier, M.; Forniés-Cámer, J.; Toupet, L.; Réau, R. *Organometallics* **2000**, *19*, 553–562. (c) Spencer, L. P.; Altwer, R.; Wie, P.; Gelmini, L.; Gauld, J.; Stephan, D. W. *Organometallics* **2003**, *22*, 3841–3854. (d) Kocher, N.; Leusser, D.; Murso, A.; Stalke, D. *Chem. Eur. J.* **2004**, *10*, 3622–3631. (e) Boubekeur, L.; Ricard, L.; Mézailles, N.; Le Floch, P. *Organometallics* **2005**, *24*, 1065–1074. (f) Co, T. T.; Shim, S. C.; Cho, C. S.; Kim, T.-J.; Kang, S. O.; Han, W.-S.; Ko, J.; Kim, C.-K. *Organometallics* **2005**, *24*, 4824–4831.

(11) Related Cp-phosphazene zirconium and lutetium complexes were reported to adopt η^5 coordination with phosphazene–metal interaction: (a) Truflandier, L.; Marsden, C. J.; Freund, C.; Martin-Vaca, B.; Bourissou, D. *Eur. J. Inorg. Chem.* **2004**, 1939–1947. (b) Rufanov, K. A.; Petrov, A. R.; Kotov, V. V.; Laquai, F.; Sundermeyer, J. *Eur. J. Inorg. Chem.* **2005**, 3805–3807.

(12) For recent reviews on η^1 -fluorenyl and η^1 -indenyl complexes, see: (a) Alt, H. G.; Samuel, E. *Chem. Soc. Rev.* **1998**, *27*, 323–329. (b) Stradiotto, M.; McGlinchey, M. J. *Coord. Chem. Rev.* **2001**, *219–221*, 311–378. (c) Kirillov, E.; Saillard, J.-Y.; Carpentier, J.-F. *Coord. Chem. Rev.* **2005**, *249*, 1221–1248.

Scheme 1. Synthesis and Coordination of the Fluorenyl-phosphazene 2

ligand **2** adopts in solution the tautomeric phosphazene form ($\text{N}=\text{P}-\text{CH}$) rather than the P-ylide form ($\text{NH}-\text{P}=\text{C}$).¹⁵ Indeed, the CH signal observed at 49.8 ppm in the ^{13}C NMR spectrum is attributed to the central C9 atom of the fluorenyl moiety and associated in the ^1H NMR spectrum to a doublet signal ($^2J_{\text{HP}} = 24.0$ Hz) at 5.09 ppm. Single crystals of **2** were obtained at -25 °C from a toluene/THF solution. X-ray diffraction analysis indicated that the same form is adopted in the solid state, since the hydrogen atom at C9 could be located and refined without any constraint (Figure 1a).

The coordination properties of the $(\text{FluPPH}_2\text{NPh})^-$ ligand toward Rh(I) were then investigated. After deprotonation with *n*-butyllithium, **2** was reacted with 0.5 equiv of $[\text{Rh}(\mu\text{-Cl})(\text{nbd})_2]$ (nbd = norbornadiene) in tetrahydrofuran. The resulting com-

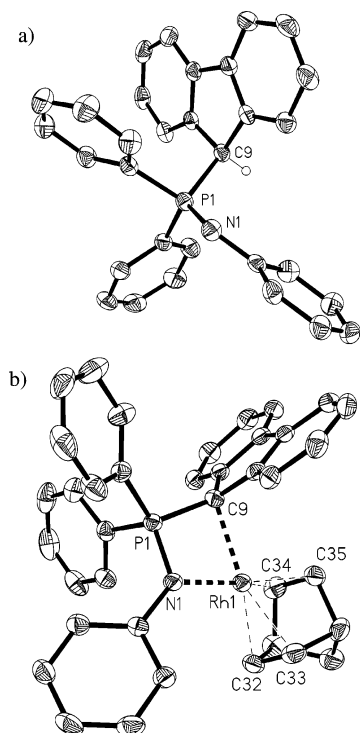
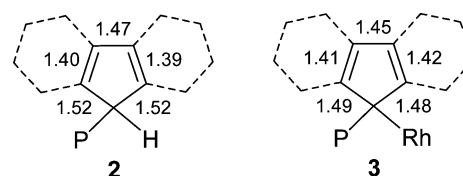


Figure 1. Molecular views of **2** (a) and **3** (b) in the solid state (hydrogen atoms are omitted for clarity). Selected bond lengths (Å) and angles (deg): **2**: P1–N1 1.5679(19); P1–C9 1.856(2); N1–C9 1.394(3); N1–P1–C9 116.70(10); C10–C9–C11 102.46(18); C10–C9–P1 109.99(15); C11–C9–P1 113.89(15). **3**: Rh1–N1 2.123(2); Rh1–C9 2.188(3); P1–N1 1.620(2); P1–C9 1.768(3); N1–Rh1–C9 74.40(9); N1–P1–C9 100.51(12); C10–C9–C11 105.2(2); C10–C9–P1 118.2(2); C11–C9–P1 126.4(2).

Chart 2. CC Bond Lengths within the Central Five-Membered Rings of the Fluorenyl Moieties in 2 and 3

plex **3** was isolated in 90% yield following extraction with dichloromethane. The ^{31}P NMR spectrum of **3** consists of a doublet signal ($J_{\text{PRh}} = 16.2$ Hz) deshielded by 16.3 ppm compared to that of **2**. The ^1H NMR spectrum features the typical signals for the $(\text{FluPPH}_2\text{NPh})^-$ and nbd ligands in a 1:1 ratio. While the mass and ^1H and ^{31}P NMR spectra are consistent with the general formula $[(\text{FluPPH}_2\text{NPh})\text{Rh}(\text{nbd})]$, they do not reveal the coordination mode of the $(\text{FluPPH}_2\text{NPh})^-$ ligand. In ^{13}C NMR, the C9 atom resonates at 33.9 ppm as a doublet of doublets ($^1J_{\text{CP}} = 109.3$ and $^1J_{\text{CRh}} = 10.5$ Hz), while the other Flu quaternary carbon atoms appear as singlets at more than 130 ppm. This suggests a low Flu hapticity, which was unambiguously confirmed by an X-ray diffraction study (Figure 1b). The rhodium center of **3** adopts a square planar arrangement, the $(\text{FluPPH}_2\text{NPh})^-$ ligand being coordinated to the metal center via the nitrogen and C9 atoms. The four-membered ring NPCRh is nearly planar (maximum deviation from the best fit plane of 0.18 Å for P). The Rh–N and Rh–C9 bond lengths (2.123 and 2.188 Å, respectively) are comparable to those observed for the related 1-aza-2-phospha(V)allyl complex $(\text{H}_2\text{CPPH}_2\text{NAr})\text{Rh}(\text{cod})$.^{4a} This $\kappa^2\text{-N,C}$ coordination is accompanied by a contraction of the PC distance (from 1.856 Å in **2** to 1.768 Å in **3**), an elongation of the PN distance (from 1.567 Å to 1.620 Å), and a noticeable decrease in the NPC bond angle (from 116.7° to 100.5°), revealing the delocalized character of the anionic ligand and the geometry constraint of the ensuing complex.¹⁶ Notably, the CC bond lengths of the central five-membered ring of the fluorenyl moiety do not equalize upon coordination and remain very similar to those observed for **2** (Chart 2). This observation suggests that the fluorenyl π -system remains fairly localized, in agreement with an $\eta^1\text{-Flu}$ coordination. This unusual bonding situation is further substantiated by the noticeable pyramidalization of the C9 atom ($\Sigma\text{C9}_\alpha = 349.8^\circ$)¹⁷ and by the remoteness of the other C_{Flu} atoms from the rhodium center (RhC distances > 3 Å). To the best of our knowledge, complex **3** is the first $\eta^1\text{-fluorenyl}$ rhodium adduct to be structurally characterized, and its selective formation over the corresponding $\eta^5\text{-complex 3'}$ (Figure 2) illustrates the ability of the short phosphazene sidearm to enforce low Flu hapticity, despite the associated geometry constraint.^{18,19}

To gain further insight into the low hapticity of the fluorenyl ring encountered in complex **3**, ab initio calculations²⁰ were performed at the DFT level of theory (Table 1). The full

(13) Baiget, L.; Bouslikhane, M.; Escudié, J.; Cretiu Nemes, G.; Silaghi-Dumitrescu, I.; Silaghi-Dumitrescu, L. *Phosphorus, Sulfur, Silicon* **2003**, 178, 1949–1961.

(14) Murata, S.; Abe, S.; Tomioka, H. *J. Org. Chem.* **1997**, 62, 3055–3061.

(15) The opposite situation was encountered in the related $\text{Cp}^*\text{PMe}_2\text{NAD}$ ligand.^{11b}

(16) The dissymmetric nature of the $(\text{FluPPH}_2\text{NPh})^-$ ligand results in the nonequivalence of the two nbd carbon–carbon double bonds, which is apparent both in NMR and in X-ray. As previously observed for the related 1-aza-2-phospha(V)allyl complex $(\text{H}_2\text{CPPH}_2\text{NAr})\text{Rh}(\text{cod})$,^{4a} the higher trans influence of the carbon compared to the nitrogen atom noticeably affects the bond distances from the metal center to the midpoints of the CC double bonds (Rh–M of 2.040 and 1.981 Å in trans position to the carbon and nitrogen, respectively), but practically not those of the CC double bonds (1.380 vs 1.388 Å).

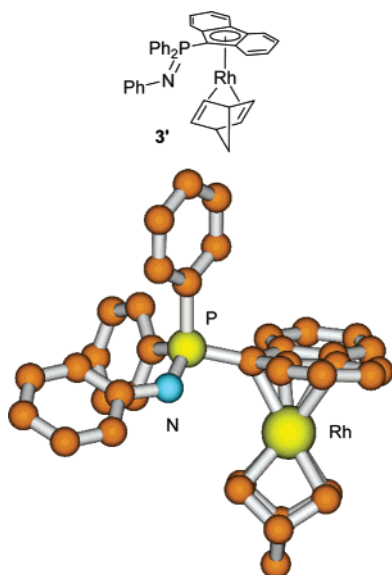


Figure 2. Optimized structure for the η^5 -complex **3'**.

substitution pattern of the NPC ligand was conserved in order to reliably take into account electronic and steric factors. Accordingly, the key features of this complex could be very well reproduced (largest deviations of only 0.04 Å for the NP and PC bond lengths and 3° for the NPC angle), indicating the capability of the method in describing this kind of system.

The bonding situation in κ^2 -N,C complexes derived from 1-aza-2-phosphaallyl ligands **A** has been described by considering the two limiting structures **a** and **b** (Chart 3).^{3a,4a} On the basis of the geometric data, complex **3** is accordingly best described by the phosphazene/alkyl structure **a**, with only minor contribution of the amido/phosphorus ylide form **b**. A more precise description could be obtained from a natural bonding analysis (NBO),²¹ especially regarding the nature of the RhC9 bond and the delocalization of the two nitrogen lone pairs (referred to as in-plane and out-of-plane, according to their orientation relative to the NPCRh metallacycle). As expected from the difference in electronegativity, the Rh—C9 bond was predicted to be polarized, but the 65% (C9)/35% (Rh) distribution indicates noticeable covalent character, in agreement with form **a**. At the second-order donor–acceptor interaction level, the nitrogen in-plane lone pair is predicted to be delocalized over empty orbitals centered at both rhodium (50 kcal·mol⁻¹) and phosphorus (20 kcal·mol⁻¹). In addition, the nitrogen out-of-plane lone pair is found to be delocalized into the phenyl ring (roughly 50 kcal·mol⁻¹), in agreement with the orientation of the phenyl ring relative to the metallacycle (twist angle of 27.1°). This NBO analysis clearly stresses the contribution of weak donor–acceptor interactions in complex **3**, resulting in a rather complicated bonding situation that is not comprehensively represented by Lewis structures **a** and **b**.

(17) The ylidic carbon center is planar in fluorenylidene phosphoranes: (a) Burford, N.; Clyburne, J. A. C.; Sereda, S. V.; Cameron, T. S.; Pincock, J. A.; Lumsden, M. *Organometallics* **1995**, *14*, 3762–3767. (b) Brady, E. D.; Hanusa, T. P.; Pink, M.; Young, V. G., Jr. *Inorg. Chem.* **2000**, *39*, 6028–6037.

(18) Introduction of a pendant phosphine sulfide has recently allowed for the first structural characterization of an η^1 -indenyl rhodium complex: (a) Wechsler, D.; McDonald, R.; Ferguson, M. J.; Stradiotto, M. *Chem. Commun.* **2004**, 2446–2447. (b) Wechsler, D.; Myers, A.; McDonald, R.; Ferguson, M. J.; Stradiotto, M. *Inorg. Chem.* **2006**, *45*, 4562–4570.

(19) For a rare example of η^5 -fluorenyl rhodium complex, see: Doppiu, A.; Englert, U.; Salzer, A. *Chem. Commun.* **2004**, 2166–2167.

(20) See Experimental Section and Supporting Information for details.

(21) Reed, A. E.; Curtiss, L. A.; Weinhold, F. *Chem. Rev.* **1988**, *88*, 899–926.

To highlight the tendency of the (FluPPh₂NPh)⁻ ligand to favor low hapticity, the related η^5 -complex **3'** has also been optimized. Its structure is represented in Figure 2, and its key geometrical parameters are listed in Table 1. Compared with the η^1 -complex **3**, the phosphazene sidearm has rotated around the C9P bond so that the nitrogen atom no longer interacts with the metal center (NRh distance of 3.88 Å). The C9Rh bond length (2.180 Å) is very similar to that calculated for **3**, and the η^5 coordination of the fluorenyl is unambiguously indicated by the close contacts predicted between the metal center and the four other carbon atoms of the central ring (RhC_(q)Flu distances ranging from 2.32 to 2.42 Å). Notably, the change of the fluorenyl hapticity from η^1 to η^5 is also accompanied by noticeable strain relief of the NPC9 bond angle (106.7°), by the equalization of CC bond lengths within the central five-membered ring (with a maximum deviation of 0.02 Å from the average value of 1.45 Å), and by the planarization of the C9 environment ($\Sigma C9_\alpha = 355.9^\circ$). In agreement with the experimental observations, the η^5 -complex **3'** has been calculated to be significantly less stable than the η^1 -complex **3**. The rather large energetic difference predicted between the two isomeric complexes (16.7 kcal·mol⁻¹) substantiates the strong influence of the phosphazene sidearm introduced on the fluorenyl, the phosphazene–rhodium interaction apparently being strong enough to compensate for the otherwise unfavorable η^1 coordination.

Conclusion

In conclusion, a fluorenyl-phosphazene ligand has been prepared and coordinated to the Rh^I(nbd) fragment. Despite the associated geometry constraint, the coordination of the short phosphazene sidearm has been demonstrated by X-ray analyses and DFT calculations to enforce low hapticity, giving thereby access to unusual η^1 -fluorenyl coordination.

Experimental Section

General Procedures. All reactions were performed using standard Schlenk techniques under an argon atmosphere. NMR spectra were recorded on Bruker Avance 300 or 400 spectrometers. ³¹P, ¹H, and ¹³C chemical shifts are expressed with a positive sign, in parts per million, relative to external 85% H₃PO₄ and TMS. Unless otherwise stated, NMR was recorded at 293 K. Elemental analyses were performed using a Perkin-Elmer 2400 (II) elemental analyzer. Mass spectra were recorded on a Hewlett-Packard 5989.

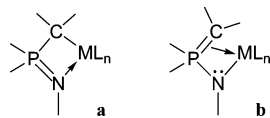
Materials and Methods. THF and toluene were dried under sodium and distilled prior to use. All organic reagents were obtained from commercial sources and used as received. [Rh(μ-Cl)(nbd)]₂ was purchased from Strem Chemicals, stocked in a glovebox, and used without further purification. The fluorenyl-diphenylphosphine **1**¹³ and phenyl azide¹⁴ were prepared according to literature procedures.

Preparation of 2 from 1. A degassed solution of PhN₃ (0.58 g, 4.8 mmol) in toluene (10 mL) was added at room temperature to a degassed suspension of Ph₂PFlu (1.34 g, 4.4 mmol) in toluene (30 mL). After stirring for 5 h, the solvent and excess of PhN₃ were eliminated under vacuum to yield a pale yellow solid. Cooling a solution of **2** in toluene/THF to -25 °C yielded 1.075 g of pale yellow crystals (56%). ³¹P{¹H} NMR (121.4 MHz, C₆D₆): δ 7.8 ppm; ¹H NMR (300 MHz, C₆D₆): δ 7.68 (d, ³J_{H,H} = 7.5 Hz, 2H, H_{1,8}), 7.42 (m, 4H, H_{15,19}), 7.34 (d, ³J_{H,H} = 7.5 Hz, 2H, H_{4,5}), 7.17 (m, 2H, H_{22,24}), 7.10 (m, 2H, H_{3,6}), 7.05 (m, 2H, H_{21,25}), 7.00 (m, 2H, H_{2,7}), 6.96 (m, 2H, H₁₇), 6.86 (m, 4H, H_{16,18}), 6.79 (m, 1H, H₂₃), 5.09 ppm (d, 1H, ²J_{H,P} = 24.0 Hz, H₉). ¹³C{¹H} NMR (75.5 MHz, C₆D₆): δ 151.7 (d, ²J_{C,P} = 3.0 Hz, C₂₀), 142.2 (d, ³J_{C,P} = 4.5 Hz, C_{11,12}), 139.7 (d, ²J_{C,P} = 3.8 Hz, C_{10,13}), 132.4 (d, ²J_{C,P} =

Table 1. Selected Bond Lengths and Angles (in Å and deg, respectively) for Derivatives **2**, **3**, and **3'**

	N–Rh	C9–Rh	N–Rh–C9	N–P	P–C9	N–P–C9	ΣC9 _a
2 (X-ray)				1.567(9)	1.856(2)	116.70(10)	326.3
3 (X-ray)	2.123(2)	2.188(3)	74.40(9)	1.620(2)	1.768(3)	100.51(12)	349.8
3^a	2.117	2.186	74.4	1.662	1.803	97.3	346.3
3^a	3.878	2.180	43.8	1.615	1.818	106.7	355.9

^a Predicted at the DFT(B3PW91) level of theory.

Chart 3. Limiting Structures for κ²-N,C Complexes Derived from 1-Aza-2-phosphaallyl Ligands

8.3 Hz, C_{15,19}), 131.2 (d, ⁴J_{C,P} = 2.3 Hz, C₁₇), 128.8 (s, C_{22,24}), 127.8 (d, ³J_{C,P} = 11.3 Hz, C_{16,18}), 127.5 (s, C_{3,6}), 127.0 (d, ³J_{C,P} = 1.5 Hz, C_{1,8}), 126.4 (d, ⁴J_{C,P} = 2.3 Hz, C_{2,7}), 123.3 (d, ³J_{C,P} = 18.9 Hz, C_{21,25}), 119.5 (s, C_{4,5}), 117.3 (s, C₂₃), 49.8 ppm (d, ¹J_{C,P} = 75.5 Hz, C₉). MS (EI, 70 eV) *m/z* (%): 441 [M]⁺, 276 [M – Flu]⁺, 165 [Flu]⁺. Mp: 243 °C. Anal. Calcd for C₃₁H₂₄NP: C, 84.35; H, 5.44; N, 3.17. Found: C, 83.80; H, 5.30; N, 3.10.

Preparation of **3 from **2**.** To a solution of **2** (95.7 mg, 0.216 mmol) in THF (6 mL) was added at –78 °C 0.144 mL of a 1.6 M solution of *n*BuLi in hexanes, and the solution was stirred 30 min at room temperature. The reaction medium was cooled to 0 °C, and a solution of [Rh(μ-Cl)(nbd)]₂ (50 mg, 0.108 mmol) in THF (3 mL) was added. After warming to room temperature and subsequent stirring for 2 h, the solvent was eliminated under vacuum. The yellow residue was extracted with CH₂Cl₂ (10 mL) and evaporated to dryness, yielding a yellow solid (123 mg, 90%). Crystals suitable for X-ray crystallography were obtained from a CHCl₃ solution at –25 °C. ³¹P{¹H} NMR (202.5 MHz, CDCl₃, 243 K): δ 24.1 ppm (d, ²J_{P,Rh} = 16.2 Hz). ¹H NMR (500.3 MHz, CDCl₃, 243 K): δ 7.98 (d, ³J_{H,H} = 7.6 Hz, 2H, H_{4,5}), 7.85 (dd, ³J_{H,P} = 11.8 Hz, ³J_{H,H} = 7.5 Hz, 4H, H_{15,19}), 7.63 (t, ³J_{H,H} = 7.0 Hz, 2H, H₁₇), 7.50 (m, 4H, H_{16,18}), 7.15–7.08 (m, 6H, H_{2,3,6,7,22,24}), 6.88 (d, ³J_{H,H} = 7.9 Hz, 2H, H_{1,8}), 6.84 (t, ³J_{H,H} = 7.3 Hz, 1H, H₂₃), 6.66 (d, ³J_{H,H} = 7.8 Hz, 2H, H_{21,25}), 4.08 (br s, 2H, H_{26,27}), 3.48 (br s, 2H, H_{30,31}), 1.47 (br s, 2H, H_{28,29}), 1.07 (d, ²J_{H,H} = 8.6 Hz, 1H, H_{32A}), 0.83 ppm (d, ³J_{H,H} = 8.6 Hz, 1H, H_{32B}). ¹³C{¹H} NMR (125.8 MHz, CDCl₃, 243 K): δ 149.5 (s, C₂₀), 141.4 (d, ²J_{C,P} = 10.1 Hz, C_{10,13}), 134.1 (d, ²J_{C,P} = 11.31 Hz, C_{11,12}), 132.60 (s, C₁₇), 132.0 (d, ²J_{C,P} = 10.7 Hz, C_{15,19}), 131.25 (d, ¹J_{C,P} = 74.8 Hz, C₁₄), 129.1 (d, ³J_{C,P} = 11.7 Hz, C_{16,18}), 128.9 (s, C_{22,24}), 123.9 (s, C_{2,7}), 121.8 (d, ³J_{C,P} = 14.0 Hz, C_{21,25}), 121.4 (s, C_{1,8}), 120.4 (s, C_{3,6}), 119.6 (s, C_{4,5}), 119.5 (s, C₂₃), 61.9 (br s, C₃₂), 58.2 (d, ³J_{C,P} = 7.8 Hz, C_{26,27}), 51.7 (d, ²J_{C,P} = 9.6 Hz, C_{28,29}), 50.3 (s, C_{30,31}), 33.90 ppm (dd, ¹J_{C,P} = 109.3, ¹J_{C,Rh} = 10.5 Hz, C₉). MS (DCI/CH₄) *m/z* (%): 636 [MH]⁺ (100), 635 [M]⁺ (75), 544 [M – COD]⁺ (4). Mp: 276 °C. Anal. Calcd for C₃₈H₃₁NPRh: C, 71.82; H, 4.90; N, 2.20. Found: C, 71.36; H, 4.83; N, 2.17.

X-ray Crystal Structures of **2 and **3**.** Data for all structures were collected at 133(2) K using an oil-coated shock-cooled crystal on a Bruker-AXS CCD 1000 diffractometer (λ = 0.71073 Å). Semiempirical absorption corrections were employed.²² The structures were solved by direct methods (SHELXS-97)²³ and refined using the least-squares method on F².²⁴ Crystallographic data (excluding structure factors) have been deposited with the Cambridge Crystallographic Data Centre as supplementary publication nos. CCDC-297701 (**2**) and 297702 (**3**). These data can be obtained free of charge via www.ccdc.cam.ac.uk/conts/retrieving.html (or from the CCDC, 12 Union Road, Cambridge CB2 1EZ, UK; fax: (+44) 1223-336-033; or deposit@ccdc.cam.ac.uk). Crystal data for **2**: C₃₁H₂₄NP, *M* = 441.48, monoclinic, space group P2₁/n, *a* = 9.4833(9) Å, *b* = 12.6243(13) Å, *c* = 19.2691(19) Å, β = 98.991(2)°, *V* = 2278.6(4) Å³, *Z* = 4, μ(Mo Kα) = 0.141 mm^{–1},

crystal size 0.2 × 0.2 × 0.5 mm³, 10 508 reflections collected (3843 independent, *R*_{int} = 0.0423), 302 parameters, *R*₁ [*I* > 2σ(*I*)] = 0.0440, w*R*₂ [all data] = 0.1130, largest diff peak and hole 0.314 and –0.302 e Å^{–3}. **3**: C₃₈H₃₁NPRh, *M* = 635.52, triclinic, space group P $\bar{1}$, *a* = 9.6858(8) Å, *b* = 11.6141(10) Å, *c* = 13.6750(11) Å, α = 106.9820(10)°, β = 94.884(2)°, γ = 96.293(2)°, *V* = 1451.2(2) Å³, *Z* = 2, μ(Mo Kα) = 0.672 mm^{–1}, crystal size 0.1 × 0.3 × 0.6 mm³, 8573 reflections collected (5880 independent, *R*_{int} = 0.0208), 370 parameters, *R*₁ [*I* > 2σ(*I*)] = 0.0353, w*R*₂ [all data] = 0.0835, largest diff peak and hole 0.603 and –0.335 e Å^{–3}.

Computational Details. Rhodium and phosphorus were treated with a Stuttgart–Dresden pseudopotential in combination with their adapted basis set.²⁵ In all cases, the basis set has been augmented by a set of polarization functions (f for Rh and d for P).²⁶ Carbon, nitrogen, and hydrogen atoms have been described with a 6-31G-(d,p) double-ζ basis set.²⁷ Calculations were carried out at the DFT level of theory using the hybrid functional B3PW91.²⁸ Geometry optimizations were carried out without any symmetry restrictions; the nature of the *extrema* (*minimum*) was verified with analytical frequency calculations. All these computations have been performed with the Gaussian 98²⁹ suite of programs. The electronic density has been analyzed using the natural bonding analysis (NBO) technique.²¹

Acknowledgment. We are grateful to the CNRS, UPS, and French Ministry of Research and New Technologies (ACI JC4091) for financial support of this work. CalMip (CNRS, Toulouse, France) is acknowledged for calculation facilities.

Supporting Information Available: Cartesian coordinates for the optimized complexes **3** and **3'**, atom numbering for the NMR assignments, and crystallographic data for derivatives **2** and **3** including cif files. This material is available free of charge via the Internet at <http://pubs.acs.org>.

OM0605377

(22) SADABS, Program for data correction, version 2.10; Bruker-AXS, 2003.

(23) Sheldrick, G. M. *Acta Crystallogr.* **1990**, *A46*, 467–473.

(24) Sheldrick, G. M. *SHELXL-97*, Program for Crystal Structure Refinement; University of Göttingen, 1997.

(25) (a) Andrae, D.; Haeussermann, U.; Dolg, M.; Stoll, H.; Preuss, H. *Theor. Chim. Acta* **1990**, *77*, 123–141. (b) Bergner, A.; Dolg, M.; Kuechle, W.; Stoll, H.; Preuss, H. *Mol. Phys.* **1993**, *80*, 1431–1441.

(26) Ehlers, A. W.; Böhme, M.; Dapprich, S.; Gobbi, A.; Höllwarth, A.; Jonas, V.; Köhler, K. F.; Stegmann, R.; Veldkamp, A.; Frenking, G. *Chem. Phys. Lett.* **1993**, *208*, 111–114.

(27) Hariharan, P. C.; Pople, J. A. *Theor. Chim. Acta* **1973**, *28*, 213–222.

(28) (a) Becke, A. D. *J. Chem. Phys.* **1993**, *98*, 5648–5652. (b) Burke, K.; Perdew, J. P.; Yang, W. *Electronic Density Functional Theory: Recent Progress and New Directions*, Dobson, J. F., Vignale, G. Das, M. P., Eds.; 1998.

(29) Frisch, M. J.; Trucks, G. W.; Schlegel, H. B.; Scuseria, G. E.; Robb, M. A.; Cheeseman, J. R.; Zakrzewski, V. G.; Montgomery, J. A.; Stratman, R. E.; Burant, J. C.; Dapprich, S.; Millam, J. M.; Daniels, A. D.; Kudin, K. N.; Strain, M. C.; Farkas, O.; Tomasi, J.; Barone, V.; Cossi, M.; Cammi, R.; Mennucci, B.; Pomelli, C.; Adamo, C.; Clifford, S.; Ochterski, J.; Petersson, G. A.; Ayala, P. Y.; Cui, Q.; Morokuma, K.; Malick, D. K.; Rabuck, A. D.; Raghavachari, K.; Foresman, J. B.; Cioslowski, J.; Ortiz, J. V.; Baboul, A. G.; Stefanov, B. B.; Liu, G.; Liashenko, A.; Piskorz, P.; Komaromi, I.; Gomperts, R.; Martin, R.; Fox, D. J.; Keith, T.; Al-Laham, M. A.; Peng, C. Y.; Nanayakkara, A.; Gonzalez, C.; Challacombe, M.; Gill, P. M. W.; Johnson, B.; Chen, W.; Wong, M. W.; Andres, J. L.; Head-Gordon, M.; Replogle, E. S.; Pople, J. A. *Gaussian 98, Revision A.11*; Gaussian, Inc.: Pittsburgh, PA, 1998.